Front. Earth Sci. 2022, 16(1): 52–63
https://doi.org/10.1007/s11707-021-0880-2

RESEARCH ARTICLE

Application of the frequency-matching method in the probability forecast of landfalling typhoon rainfall

Rong GUO (✉), Hui YU, Zifeng YU, Jie TANG, Lina BAI

Shanghai Typhoon Institute, and Key Laboratory of Numerical Modeling for Tropical Cyclone of China Meteorological Administration, Shanghai 200030, China

Abstract In this paper, a revised method for typhoon precipitation probability forecast, based on the frequency-matching method, is developed by combining the screening and the neighborhood methods. The frequency of the high-resolution precipitation forecasts is used as the reference frequency, and the frequency of the low-resolution ensemble forecasts is used as the forecast frequency. Based on frequency–matching method, the frequency of rainfall above the rainstorm magnitude increases. The forecast members are then selected by using the typhoon tracks of the short-term predictions, and the precipitation probability is calculated for each member using a combination of the neighbor and the traditional probability statistical methods. Moreover, four landfalling typhoons (i.e., STY Lekima and STS Bailu in 2019, and TY Hagupit and Higos in 2020) were chose to test the rainfall probability forecast. The results show that the method performs well with respect to the forecast rainfall area and magnitude for the four typhoons. The Brier and Brier skill scores are almost entirely positive for the probability forecast of 0.1–250 mm rainfall during Bailu, Hagupit and Higos (except for 0.1mm of Hagupit), and for < 100 mm rainfall (except for 25 mm) during Lekima.

Keywords frequency-matching method, landfalling typhoon, rainfall probability, Brier score

1 Introduction

China is severely affected by typhoons, with an average of 7–8 landfalling typhoons each year (Chen and Ding, 1979). Typhoons result in gales, rainstorms and storm surges (Chen and Xu, 2017; Yu and Chen, 2019).The main type of disaster caused by landfalling typhoons is rainstorm, which can cause flooding or the collapse of large reservoirs, resulting in serious loss of life and property (Chen and Meng, 2001; Chen et al, 2019a).

In the late 20th century, the operational forecasts of precipitation in China depended mainly on deterministic forecasts from numerical weather prediction (NWP). Since the precipitation forecast has unavoidable randomness and uncertainty compared with the forecasts of other meteorological elements, such as temperature and pressure, the precipitation probability forecast, which describes the possibility of precipitation occurrence, is more useful than the traditional deterministic forecasts (Du, 2002; Li et al., 2010; Du et al., 2018). As such, the weather forecast is inadequate if it is only a deterministic forecast with a single value (National Research Council, 2006). Ensemble numerical forecasts provide the key foundation for the change from single-value deterministic forecasts to multi-value probability forecasts (Lorenz, 1995, 1996; Li, 2002; Du, 2002; Mu and Zhang, 2006; Yamaguchi et al., 2009, 2012; Li et al., 2010, 2014a, 2014b). Therefore, in recent years, ensemble numerical forecasts have gradually become essential and been widely used, especially as an important reference for mid- and short-range weather forecasts (Yang, 2001; Chen et al., 2009; Du et al., 2014; Buizza et al., 2018).

Several statistical interpretation techniques have been developed recently, based on ensemble forecasts from NWP. In particular, for multiple ensemble members consisting of several models or parameterization schemes, some ensemble methods and post-processing techniques, such as artificial neural network, rank, bias correction, and frequency-matching methods, have been used for short-term ensemble precipitation probability forecasts, with encouraging results (Du et al., 1997; Hamill and Colucci, 1997, 1998; Hamill et al., 2010; Voisin et al., 2010; Du, 2011). Ebert (2001a, 2001b) proposed the concept of frequency-matching, which is an idea similar to the

Received July 2020; accepted February 7, 2021

E-mail: guor@typhoon.org.cn

relationship between radar reflectivity and rain rate (Rosenfeld et al., 1993). Many studies have demonstrated that the frequency-matching method calibrates the systemic errors efficiently in numerical precipitation forecasts, and can also reduce forecast errors (Ebert, 2001a, 2001b; Li et al., 2014b, 2015; Zhu and Luo, 2015). The probability-matched ensemble mean retains the accuracy of the rainfall position forecast after smoothing by the ensemble mean, and also has the advantage of the original ensemble members in the rainfall magnitude forecast (Ebert, 2001a, 2001b). Zhi et al. (2019) also found that the false ratio of light rain prediction and the missing ratio of the heavy rain prediction can be reduced by using this method for revising the multi-model rainfall forecast. By using the method, most researchers have studied on the deterministic prediction, but few on the probability forecast of landing typhoons. However, the widely used probability forecast method is the "average method", but it is usually failed to forecast the rainstorm area (Du et al., 1997; Stensrud et al., 2000; Ebert, 2001a, 2001b). So if it is necessary to have a better performance on the probability forecast operationally, we need to find out a new approach.

In this study, we developed a technique for ensemble probability forecasts based on the frequency-matching method. This method is a statistical correction, which calculates cumulative frequency distributions of reference and forecast data. A key question is what can be used as reference data. Previous studies have found that high-resolution deterministic precipitation forecasts can be relatively accurate for rainfall magnitude, but have considerable bias for rainfall area (Schwartz et al., 2010). In contrast, precipitation probability forecasts have some uncertainties, such as the rainfall area and probability of extreme rainfall. Therefore, in this paper, based on the probability matching algorithm, the deterministic precipitation forecasts are used as reference data, and the ensemble precipitation forecasts are used as forecast data. This technique not only retains the advantages of rainfall magnitude prediction from high-resolution deterministic forecasts, but also retains the uncertainty of ensemble forecasts on the prediction of rainfall area.

2 Data and methods

2.1 Data

The rainfall forecast data used in this study are from August 1st to 31st in 2019 and 2020, the daily precipitation forecasts are from the NWP of the European Centre for Medium-Range Weather Forecasts (ECWMF; EC in short hereafter). It should be noted that the precipitation forecasts from EC include deterministic and ensemble forecasts. Moreover, the typhoon tracks used here include the typhoon real-time track recording data released by the Central Meteorological Observatory of China and the typhoon track forecasts from EC Integrated Forecast System (EC-IFS), EC Ensemble Prediction Systems (EC-EPS), and Shanghai Multi-model Ensemble Forecast System (SHME).

The rainfall observation data are the 24 h accumulated amounts from 1046 surface air observation stations in China during the landfall of typhoons Lekima, Bailu, Hagupit, and Higos in August 2019 and 2020. The deterministic precipitation forecasts from EC were at 08:00 and 20:00 (Beijing time), and the spatial resolution is $0.125°\times0.125°$. The EC ensemble precipitation forecasts include 1 control member and 50 disturbance members, and the spatial resolution is $0.5° \times 0.5°$.

Typhoon track data from EC-IFS and SHME were recorded four times a day (08:00, 14:00, 20:00, and 02:00). The EC deterministic forecasts perform well in forecasting both typhoon tracks and rainfall. Compared with the EC-IFS track forecasts, the track deterministic forecast of the SHME has a similar or even smaller error for 72 h track prediction and a stable performance (Chen et al., 2019b). It is known that the typhoon track is one of the most critical factors affecting the forecasting of typhoon rainfall. Thus, in terms of the short-term predictions, the SHME forecasts can be used for selecting ensemble members of precipitation forecast, combined with the precipitation distribution.

2.2 Methods

2.2.1 Frequency-matching method

The basic principle of the frequency-matching method is that, by counting the reference frequencies and forecast frequencies of the rainfall occurrence at different rainfall thresholds, the forecast frequencies with bias are adjusted to be consistent with the reference frequencies at the same rainfall grades (Ebert, 2001a, 2001b; Li et al., 2014b, 2015). The specific method is as follows.

- Calculate the two sets of statistical data for reference precipitation frequency (i.e., *PF*) and forecast *PF* (Fig.1), which is expressed as

$$PF_i = \frac{NP_i}{NP}, \tag{1}$$

where PF_i denotes the precipitation frequency at a given threshold, NP_i is the total number of grid points where rainfall occurs per day at a given threshold, *NP* is the total number of grid points per day, and *i* is a given threshold. If we divide the precipitation thresholds into 0.1, 1, 5, 10, 15, 25, 50, 75, 100, 150, 200, 250, and 300 mm, then the corresponding *i* is 1, 2, 3,...,13.

- Calculate the cumulative probability (i.e., *CP*) at different precipitation thresholds. Cumulative Probability is the sum of the probabilities of all possible values in certain interval, such as cumulative probability of 100 mm is to calculate all the values from 0 mm to 100 mm, which

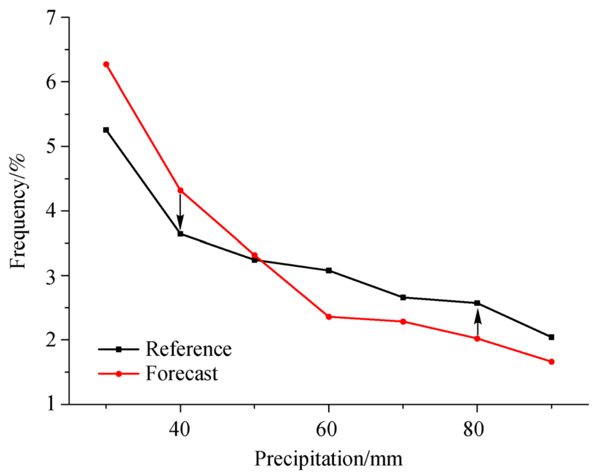

Fig. 1 The concept of the frequency-matching method.

is expressed as

$$CP_i = \sum\nolimits_{t=1}^{i} PF_t, \tag{2}$$

where CP_i is the cumulative probability at a given threshold i, such as a CP of 50 mm of precipitation (according to the first step) and $CP_7 = PF_1 + PF_2 + \cdots + PF_7$.

- The forecast frequency distribution is adjusted to be consistent with the reference frequency distribution, as follows:

$$CP_{\mathrm{r}}(i) = A_i CP_{\mathrm{f}}(i), \tag{3}$$

where CP_{r} is the reference CP and CP_{f} is the forecast CP. We can then calculate the correction coefficients A_i. The correction coefficients for any precipitation can finally be estimated by interpolation.

- Calculate the precipitation forecast after frequency-matching as follows:

$$P_{\mathrm{cf}}(i) = A_i P_{\mathrm{f}}(i), \tag{4}$$

where P_{cf} is the precipitation forecast after frequency-matching and P_{f} is the original ensemble forecast.

By using this method to revise the multi-model rainfall forecast, it can be found that the false ratio of light rain prediction and missing ratio of heavy rain prediction can be reduced (Zhi and Lyu, 2019). Therefore, by using this method to correct typhoon rainfall forecasts we expect to improve the forecast performance for heavy rainfall.

2.2.2 Extracting forecast probability: a “neighborhood” approach

In traditional ensemble forecast methods, it is assumed that all ensemble members have the same skills and weights. In addition, for any member, it is binary probability. For example, given a threshold q, the binary probability of a single grid point is as follows (Craig et al., 2010; Ebert, 2008):

$$BP_{ki} = \begin{cases} 1 & \text{if } F_{ki} \geqslant q \\ 0 & \text{if } F_{ki} < q \end{cases}. \tag{5}$$

The traditional equation for ensemble probability forecast is as follows:

$$EP_i = \frac{1}{n} \sum\nolimits_{k=1}^{n} BP_{ki}. \tag{6}$$

Here n denotes the number of the ensemble members, k denotes the kth ensemble member, and i denotes the ith grid point.

The principle of the ensemble forecast based on the neighborhood method is that, first,the values of all grid points within a predefined spatial range are used to form an ensemble forecast, and then an ensemble mean is calculated by the values of these grid points,which represents the rainfall probability at the center of the range.

The equation for the rainfall probability obtained at the center (Fig. 2) by applying the neighborhood method is as follows:

$$NP_{ki} = \frac{1}{N_b} \sum\nolimits_{m=1}^{N_b} BP_{km}, \tag{7}$$

where N_b denotes the number of grid points within r near the center, and P_{km} represents the rainfall probability at each grid point. The grid points in Fig. 2 with rainfall amount greater than or equal to threshold q are gray and are considered to have a rainfall probability value of 1.The range radius r is set to 2.5 times the original grid interval, and the probability of rainfall amount q occurring at the center point is calculated as 38%, namely, NP_i = 38% (Fig. 2).

In this paper, we combine the traditional ensemble probability forecast method with the neighborhood method. When the neighborhood method is applied to

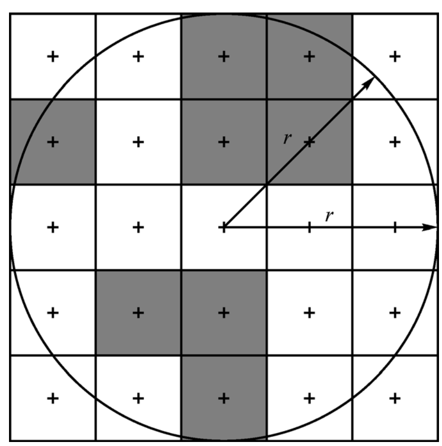

Fig. 2 Schematic example of neighborhood determination and fractional creation for a model forecast. Here a radius of 2.5 times the grid length is specified.

each ensemble member, a set of NP_i grids are generated. The ensemble rainfall probability is calculated as follows:

$$NEP = \frac{1}{n}\sum\nolimits_{k=1}^{n} NP_{ki}, \tag{8}$$

where k denotes kth ensemble member, and NP_{ki} denotes the ensemble probability value of a single ensemble member.

2.2.3 Ensemble member screening method

A previous study that evaluated the typhoon forecast accuracy during 2016–2017 (Chen et al., 2019b) showed that SHME has an advantage over the objective short-term track forecast. Therefore, the tracks of SHME are used here for selecting the ensemble members, which can effectively filter out some members that are too far from the relative truth values. Figure 3 shows the principle of the screening method, and our target was to get ensemble members available around the tracks from SHME (the members may be different under the different forecast leading time); i.e., by selecting the EC ensemble members in the black circle in Fig. 3. The specific process is as follows:

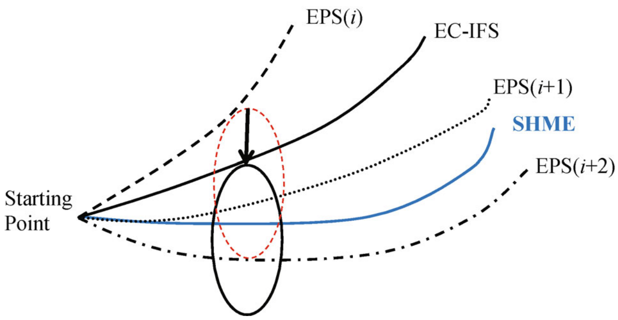

Fig. 3 Ensemble member screening of the precipitation probability forecast. Solid blue, dotted black, and solid black lines represent the typhoon tracks from SHME, EC–EPS, and EC–IFS, respectively. Red and black circles denote the typhoon track dispersion of EC–EPS and after screening of SHME, respectively.

- First, the typhoon track dispersion from EC-EPS is calculated from the 51 members. There are three steps: 1) We first check the storm motion in 24 h, and then determine the location at 0, 6, 12, 18, 24 h; 2) We then obtain the edges of several locations, such as the easternmost ($L_{\rm e}$) and westernmost ($L_{\rm w}$) sides of the northward storm at certain times (forecast times of 0, 6, 12, 18, 24h); 3) Finally, we obtain the dispersion of the upper and lower boundary (i.e., the blue and dotted black track, respectively), and all EC-EPS members should be included in this range (Fig. 4):

$$\Delta L_i = L_{i\rm e} - L_{i\rm w}, \tag{9}$$

where i is for different forecast time.

- Second, we computed the difference (ΔD) in the track forecast from EC-IFS and SHME. This generates a new $\overline{L}_{i\rm e}$

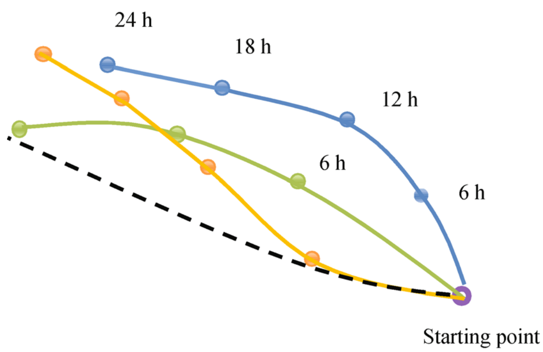

Fig. 4 Calculation of the typhoon track dispersion. Each line shows a track of a different member from EC-EPS.

and $\overline{L}_{i\rm w}$:

$$\overline{L}_{i\rm e} = L_{i\rm e} + \Delta D, \tag{10}$$

$$\overline{L}_{i\rm w} = L_{i\rm w} + \Delta D. \tag{11}$$

- Finally, we picked the members from EC-EPS located in the range between $\overline{L}_{ie}$ and $\overline{L}_{iw}$.

The main purpose of this step is to calculate the typhoon track dispersion and screen ensemble members to obtain a more probable rainfall distribution by using more accurate typhoon track forecasts.

2.2.4 Verification metrics — brier score and brier skill score

Brier scores (BS; Brier, 1950; Murphy, 1973) are commonly used to test the performance of a probability forecast, similar to the mean-square deviation of a single prediction score. The BS can be regarded as a measure of the revision of a set of probability forecasts. The lower the BS of a set of predicted values, the better the revision. The equation for obtaining the BS is as follows:

$$BS = \frac{1}{N}\sum\nolimits_{i=1}^{N} (p_i - o_i)^2, \tag{12}$$

where p_i denotes the probability of prediction, o_i the actual probability, and N the number of events predicted. Brier skill scores (BSS; Stefanova and Krishnamurti, 2002; Bradley et al., 2008; Li et al., 2010) is defined as follows:

$$BSS = \frac{BS_{\rm ct1} - BS_{\rm fst}}{BS_{\rm ct1}}. \tag{13}$$

3 A precipitation probability forecast based on the frequency-matching method

3.1 Frequency-matching of typhoon rainfall

In this section, the daily precipitation data (24 h accumulated amount)from EC-IFS and EC-EPS from 0°N–50°N and 90°E–135°E in August 2019 and 2020 were selected. The rainfall amount from 1 to 500 mm was divided into 5 mm intervals, thus 102 rainfall thresholds were obtained (the first and second thresholds were set to 0.1 and 1, respectively). It is necessary to count the frequency distribution, according to these thresholds. The PF from EC-IFS is set as the reference frequency, and the frequency from EC-EPS is set as the forecast frequency.

Figure 5(a) shows the PF at 08: 00 on August 10, 2019, and it can be found that the *PF* from EC-EPS at each threshold is considerably less than that from EC-IFS. Compared with EC-IFS, there are some significant lower frequency areas (dry biases) in the EC-EPS precipitation forecasts. The transformation coefficients were obtained according to the method outlined in Section 2.2.1. Figure 5(b) shows the transformation coefficients at each threshold for the 24 h forecast on August 10 based on the frequency-matching method (i.e., by adjusting the PF from EC–EPS to be comparable with the PF from EC–IFS). This suggests that if the frequencies from EC-IFS are less than those from EC-EPS, the transformation coefficients are < 1; otherwise, the transformation coefficients are > 1 (Fig. 5(b)). The *PF* at the thresholds of 100–200 mm has significant biases, and the corresponding transformation coefficients deviate considerably from 1, and thus the adjustment magnitude (that is adjustment of precipitation forecast) is large. Moreover, the frequency from EC-EPS for large rainfall amounts of > 250 mm is close to that of EC-IFS, and the corresponding transformation coefficients are close to 1, thus, the adjustment magnitude is small.

Furthermore, according to the transformation coefficients calculated at each threshold, the interpolation method was used to obtain the transformation coefficients for any rainfall amount (Fig. 5(b)). At the same time, the revised rainfall can be obtained by using the transformation coefficients multiplied by the original rainfall at the corresponding grid points. In general, the EC ensemble precipitation forecasts can be adjusted by the transformation coefficients (Eq. 4).

It is evident that the frequency of light rain (< 50 mm) decreases, and the frequency and magnitude of heavy rain (> 100 mm) increase after revision by the frequency-matching method (Fig. 6).

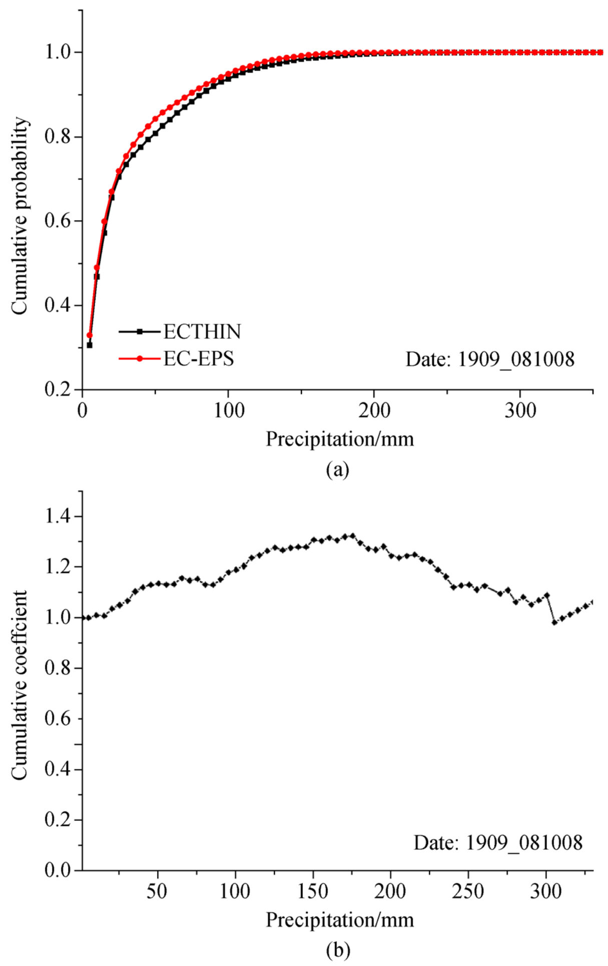

Fig. 5 (a) PF at 08:00 on August 10, 2019 under different thresholds (black line: CP of EC-IFS; red line: CP of EC-EPS), and (b) the corresponding transformation coefficients.

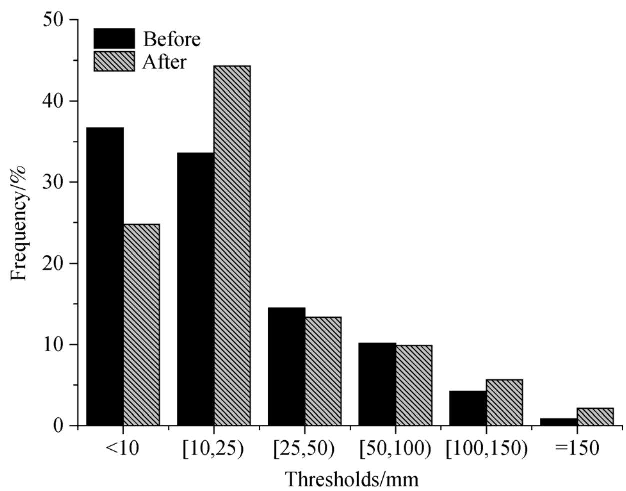

Fig. 6 Precipitation rate before and after the revision at 08:00 on August 10, 2019.

3.2 Ensemble members screening by the multi-model ensemble track

The screening method is dependent on the bias of the EC–IFS and SHME track forecasts, and the SHME track is based on a real-time correction method. As such, if there is little difference in the mean track error, then the selective members will not be reduced. Table 1 shows the results of the ensemble member screening.

The screening method eliminates several members during typhoons Lekima and Bailu (20%–40%), but not for Hagupit and Higos. This is mainly because the track

Table 1 Ensemble members after track screening

TC Name	Lekima	Bailu	Hagupit	Higos
Total members	49	49	51	51
Selective members	39	29	50	48

forecasts from EC–IFS and SHME are close to true values (Table 1).

3.3 Rainfall probability-forecast experiment during typhoon the landfall of Lekima and Bailu

In order to test the performance of the previously proposed rainfall probability method on the rainfall area and amount during a landfalling typhoon, this section focuses on the heavy rainfall during landfall of Lekima and Bailu. The periods selected for study are from 08:00 on August 10 to 08:00 on August 11, 2019 for Lekima, and 08:00 on August 25 to 08:00 on August 26, 2019 for Bailu. Hagupit and Higos yielded similar conclusions to these two case studies.

3.3.1 Lekima

Figure 7 shows the 24 h rainfall probability forecast at each grade from 08:00 on August 10 to 08:00 on August 11

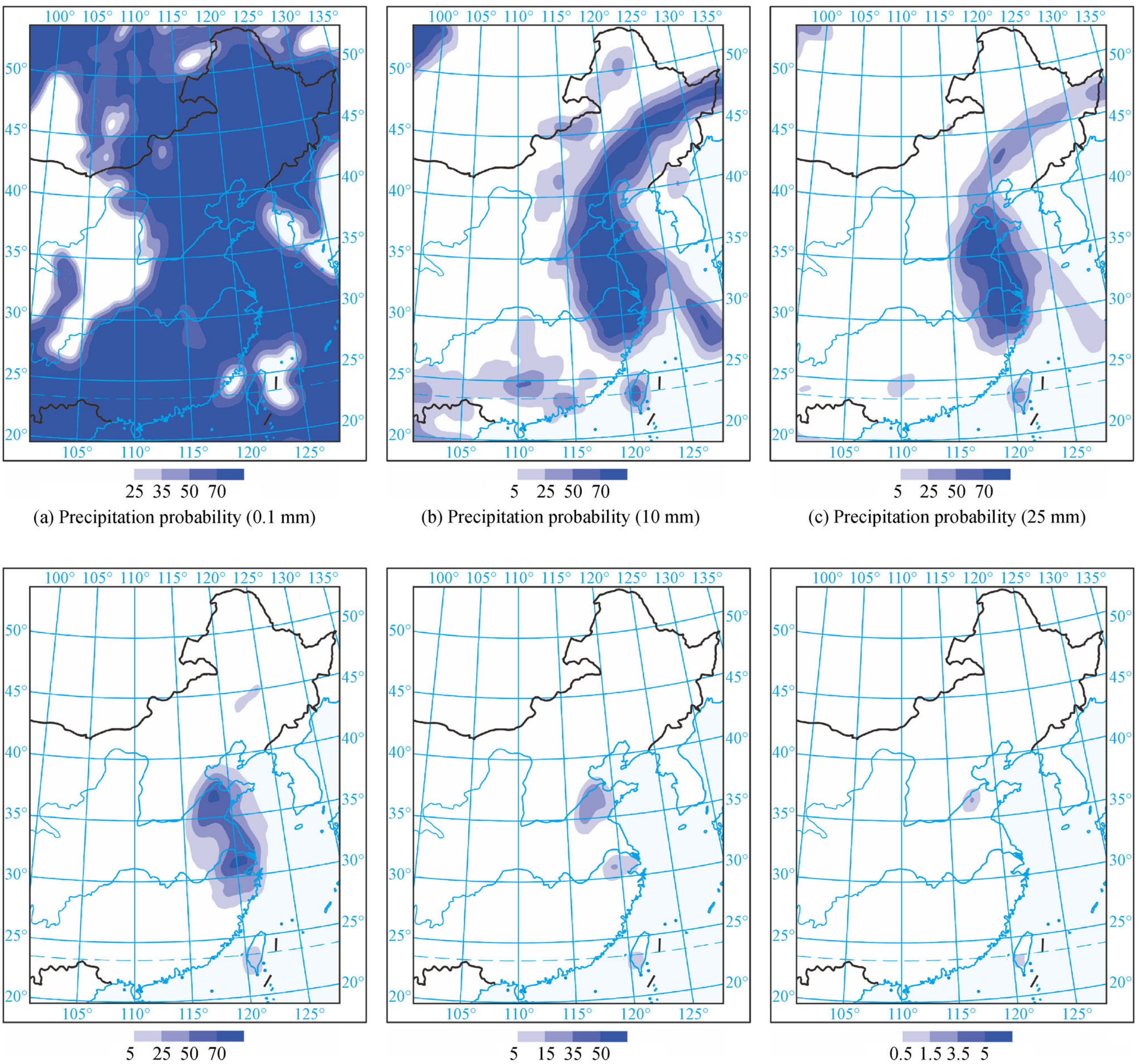

(a) Precipitation probability (0.1 mm) (b) Precipitation probability (10 mm) (c) Precipitation probability (25 mm)

(d) Precipitation probability (50 mm) (e) Precipitation probability (100 mm) (f) Precipitation probability (250 mm)

Fig. 7 24 h rainfall probability forecast at 00:00 on August 10, 2019 at the thresholds of 0.1, 10 25, 50, 100 and 250 mm.

during the impact of the super typhoon Lekima (No. 1909). For the 0.1 mm rainfall, in east China and south China, the occurrence probability of rainfall exceeds 70%. For the 10 mm rainfall, the rainfall area reduces considerably from that of 0.1 mm, and the occurrence probability is < 5%, except for most of Zhejiang, northern Fujian, eastern Jiangxi, most of Jiangsu, Shanghai and eastern Shandong regions, where there is > 70% probability of > 10 mm of rainfall. These areas can be considered to have a higher probability for more significant rainfall. For the 25 mm rainfall, the heavy rain is concentrated mainly in Zhejiang, Shanghai, the eastern coast of Shandong, and southern Zhejiang regions, with a probability of > 25%. For the 50 mm rainfall, the results show that there is still a 25% probability in northern Zhejiang, Shanghai, and most of Jiangsu and Shandong regions. Moreover, rainfall above 100mm is mainly located in central Shandong and eastern Jiangsu regions, with a 15%–35% probability. A previous application of the probability forecast has shown that a warning is required when the forecast probability of a rainstorm of > 50 mm exceeds 30%, and there is high probability of a heavy rainstorm.

Figure 8 shows that the rainfall areas of 10 and 25 mm after revision are generally consistent with the observations, and are closest to the observations when the probabilities are 50% and 25%. The revised 50 mm rainfall probability forecast is also similar to the observations, and is also the most accurate when the probability is 25%. However, there is a > 25% probability of rainstorm in southwestern Shandong Province, which is a false prediction. For a heavy rainstorm above 100 mm, the probability forecast with a 5% rainfall probability is closest to the observations, and there are smaller biases in eastern Jiangsu and Shanghai regions, and a missed prediction in

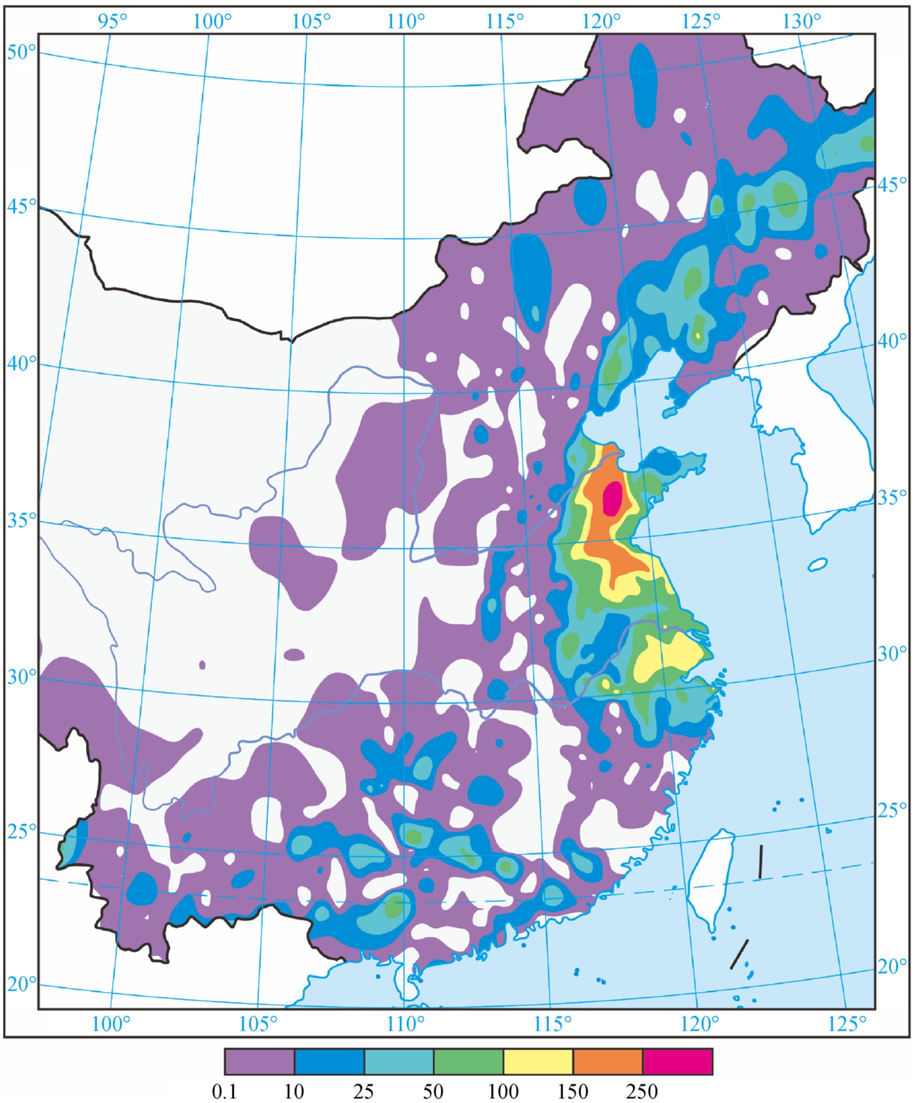

Fig. 8 Distribution of observational rainfall during Lekima from 08:00 on August 10 to 08:00 on August 11 (interpolated from air observation station data).

northern Jiangsu Province. The probability of rainfall above 250 mm is small and close to 1%.

3.3.2 Rainfall probability-forecast during the typhoon Bailu

Figure 9 shows the 24 h rainfall probability forecast at each grade from 08:00 on August 25 to 08:00 on August 26, 2019 during the severe tropical storm Bailu (No. 1911). For the 0.1 mm rainfall, there is a 70% occurrence probability in the middle and lower reaches of the Yangtze River, and most of Guangdong, coastal areas of Fujian, and most of Guangxi regions. For the 10 mm rainfall, there is a 50% occurrence probability in most of Guangdong and Fujian provinces. For the 25 mm rainfall, there is an approximately 25% occurrence probability in most of Guangdong, southwest of Fujian, and southeast Guangxi regions. Moreover, for the 100 mm rainfall, the rainfall area is small, and the 25% probability is concentrated mainly in Guangdong Province.

Figure 10 shows the distribution of observational rainfall during Bailu. For the revised probability forecasts of 0.1, 10 and 25 mm rainfall, the rainfall areas are generally consistent with the observations, and are closest to the observations when the probabilities are 95%, 50%, and 25%. For the 50 mm rainfall, the revised rainfall area is

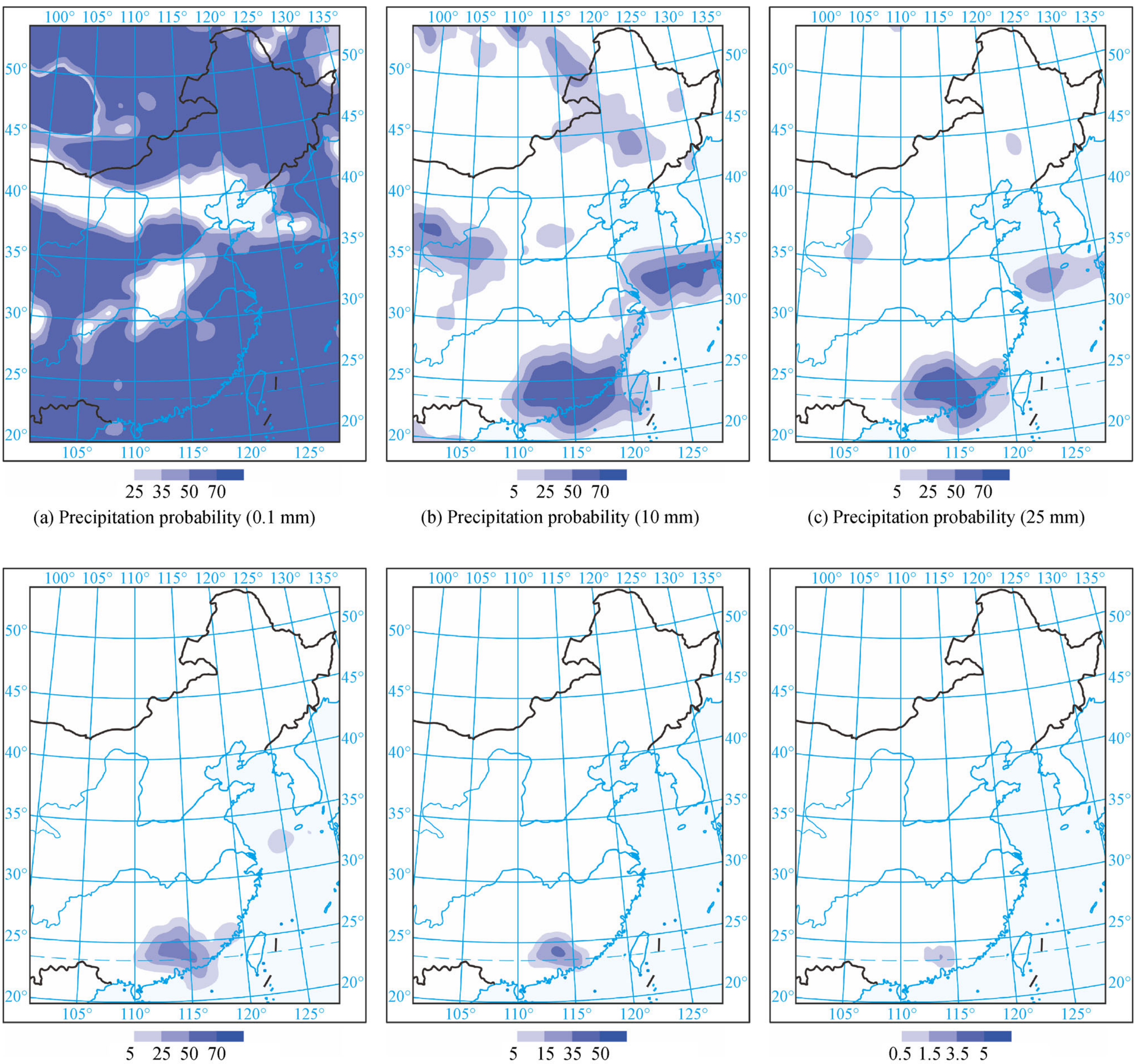

(a) Precipitation probability (0.1 mm) (b) Precipitation probability (10 mm) (c) Precipitation probability (25 mm)

(d) Precipitation probability (50 mm) (e) Precipitation probability (100 mm) (f) Precipitation probability (250 mm)

Fig. 9 24 h rainfall probability forecast at 00:00 on August 25, 2019, at the thresholds of 0.1, 10, 25, 50, 100, and 250 mm.

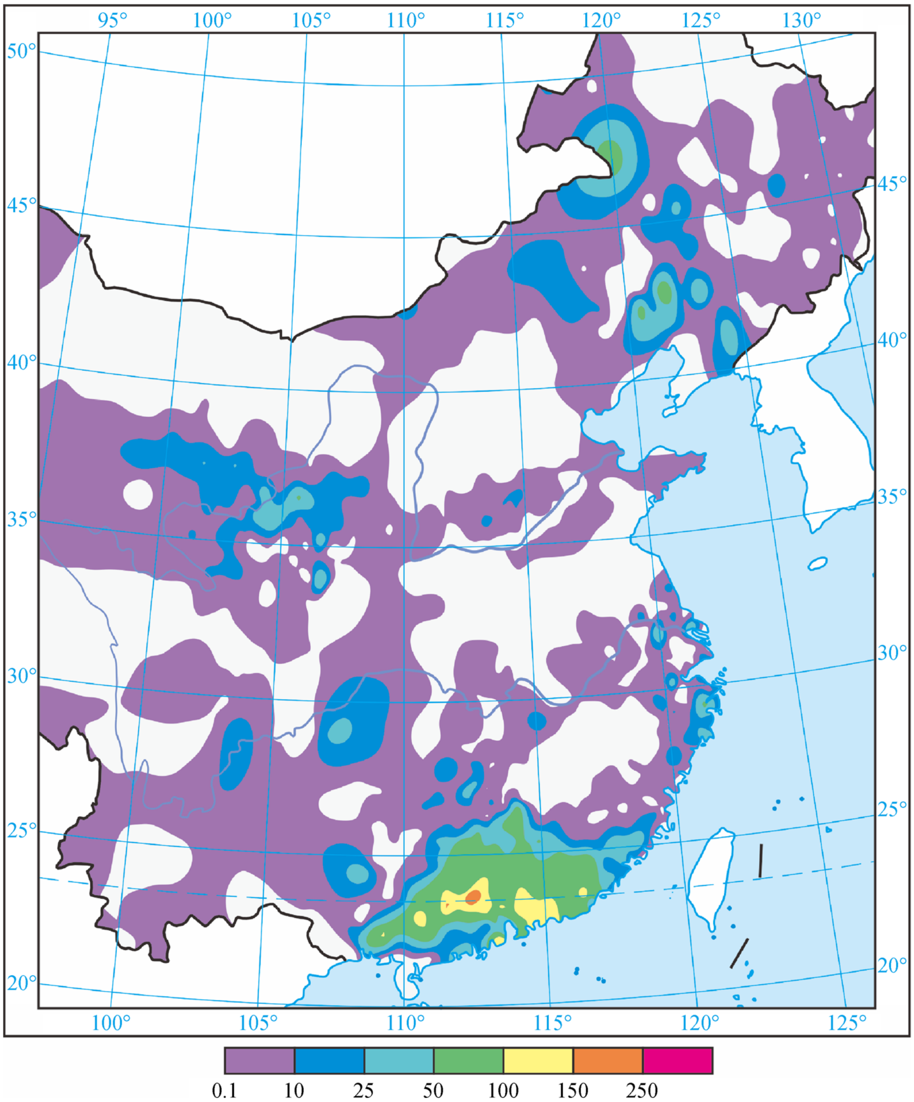

Fig. 10 Distribution of observational rainfall during Bailu from 08:00 on August 25 to 08:00 on August 26, 2019.

most similar to observations in both form and location when rainfall probability is 25%, but there is a missed prediction in eastern Zhejiang Province. For a heavy rainstorm above 100 mm, there are two centers of extreme rainfall with a rainfall probability of ~5%, and the result is consistent with the observations. The probability of rainfall above 250 mm is small (~1%).

3.4 Precipitation probability-forecast for Lekima, Bailu, Hagupit and Higos

At present, the most commonly used probability forecast method on operation is the “average method”, that is, giving each ensemble member the same weight (Stensrud et al., 2000; Du et al., 1997; Ebert, 2001a, 2001b). And this method has already been introduced as traditional ensemble forecast method (see Section 2.2.2).

In this paper, the precipitation forecast from EC-EPS before revision was used as the reference forecast during the testing process. If the *BSS* is > 0, there is a positive skill; otherwise, there is a negative skill.

Table 2 presents the results of the BS before and after the precipitation probability is revised. The results suggest that the *BS* are all $< 20\%$ during Lekima landfall. In the forecast experiment for the first period, the model with the revised method provides a slightly improved precipitation probability forecast compared with the original model, which is only slightly worse than the original model for rainfall greater than 250 mm. In the forecast experiment for the second period, the revised method is slightly worse than the original model for the 25 mm rainfall probability, and equal to or slightly better than the original model for the probability forecast of the other rainfall grades. During Bailu landfall, the revised method provides more significant improvements in both the 0.1 and 10 mm precipitation probability forecasts. In the forecast experi-

Table 2 Brier scores after and before the revision

	Grid number	0.1 mm		10 mm		25 mm		50 mm		100 mm		250 mm	
		CR	OR	CR	OR	CR	OR	CR	OR	CR	OR	CR	OR
1909	478	0.14	0.18	0.15	0.16	0.18	0.19	0.14	0.15	0.09	0.09	2.6e-6	0
	474	0.17	0.20	0.11	0.13	0.07	0.06	0.09	0.10	0.03	0.03	0	0
1911	398	0.25	0.49	0.16	0.32	0.10	0.22	0.05	0.12	7e-3	3e-2	6e-5	6e-5
	504	0.23	0.26	0.13	0.10	0.12	0.10	0.09	0.10	1.9e-2	2.4e-2	2.6e-6	6e-5
2004	500	0.53	0.46	0.15	0.24	0.07	0.12	0.06	0.09	2.8e-2	3.2e-2	8e-3	8e-3
2007	300	0.41	0.48	0.34	0.42	0.19	0.25	0.08	0.07	3.6e-4	1.9e-4	0	0
	396	0.37	0.44	0.28	0.46	0.21	0.34	0.12	0.16	8e-3	1e-2	0	0

ment for the first period, the area of rainfall above 250 mm is small, and the revision has not improved the probability forecast. In addition, in the forecast experiment for the second period, the probability forecast of the rainfall above 100 mm is improved considerably after the revision. During Hagupit landfall, the revised method provides significant improvements except at a threshold of 0.1 mm, and there is also a better performance for the Higos landfall. In the first period of Higos landfall, rainfall was limited. The revised method is 15%–25% better than the reference forecast in the 0.1, 10, and 25 mm thresholds. In the second period, with heavy rainfall, the BS of the revised method is much better than that of the reference forecast for each threshold.

Figure 11 shows that the revised method for the probability forecast of landfalling typhoon rainfall based on the frequency-matching method performs better during Bailu, Hagupit and Higos. There are mostly positive skill scores for the rainfall probability forecasts from 0.1 to 250 mm, and an obvious improvement in the 100 mm and 250 mm precipitation probability forecast for Bailu. During Lekima, there are positive skill scores for the rainfall probability forecasts of 0.1, 10, and 50 mm, but not for rainfall above 100 mm. There is a negative skill score for the 25 mm rainfall probability forecast.

From the precipitation probability forecast experiments, it can be concluded that the revised method improves the forecast more significantly when the original model performs poorly. However, the improvement is limited when the original model forecasts well.

4 Discussion and conclusions

Based on the frequency-matching method, we presented a revised approach for typhoon rainfall probability forecast using the screening and neighborhood methods. This method was tested with rainfall probability forecasts during the landfalls of Lekima, Bailu, Hagupit and Higos.

The frequency of the high-resolution deterministic precipitation forecast was used as the reference frequency, and the frequency of the low-resolution ensemble precipitation forecast was used as the forecast frequency. The frequency-matching method increased the *PF* of heavy rainfall and decreased the *PF* of light rain.

The screening method for the typhoon track from the multi-model ensemble forecast can effectively filter out 20%–40% of the ensemble members for Lekima and Bailu, which can preserve the uncertainty of the ensemble forecast, and effectively filter out the members that deviate

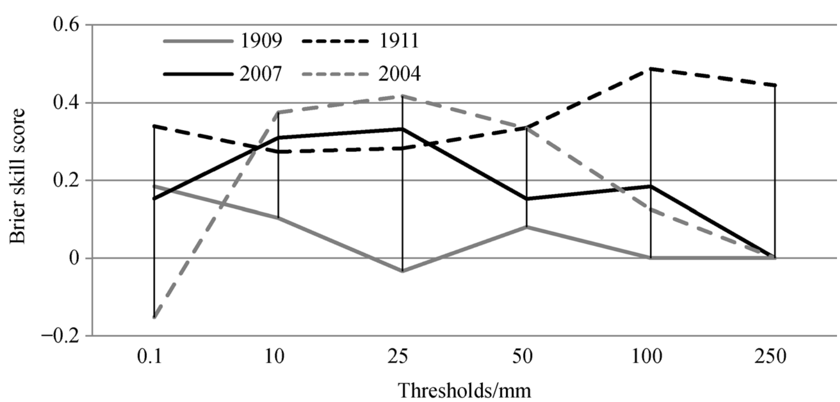

Fig. 11 Brier skill scores of the revised rainfall probability forecast for the landfalls of Lekima, Bailu, Hagupit, and Higos (gray line = Lekima; black dashed line = Bailu; black line = Higos; gray dashed line = Hagupit).

from actual values. For Hagupit and Higos, the effects of screening are unsatisfactory, because the track forecast error is limited.

The rainfall probability forecast experiment during the landfall of the four typhoons suggests the revised method predicts the rainfall area and amount well, but not the 250 mm rainfall probability forecast. Moreover, the *BS* of rainfall probability forecasts for Lekima and Bailu were low, and the revised method for the rainfall probability forecast of 0.1, 10 and 50 mm were all good. For the *BSS*, except for the 25 mm rainfall during Lekima and 0.1 mm rainfall during Hagupit, there were mostly positive skill scores. Therefore, the revised method can improve the probability forecast of landfalling typhoon.

Acknowledgements This research was funded by the Key Program for International S&T Cooperation Projects of China (No. 2017YFE0107700), the National Natural Science Foundation of China (Grant Nos. 41875080, 41775065), the Research Program from Science and Technology Committee of Shanghai (Nos. 19dz1200101, 20ZR1469700), the National Key R&D Program of China (2020YFE0201900), and in part by Shanghai Typhoon Innovation Team grants to Shanghai Typhoon Institute.

References

Bradley A A, Schwartz S S, Hashino T (2008). Sampling uncertainty and confidence intervals for the Brier score and Brier skill score. Weather Forecast, 23(5): 992–1006

Brier G W (1950). Verification of forecasts expressed in terms of probability, Mon Wea Rev, 78: 1−3

Buizza R, Du J, Toth Z, Hou D (2018). Major operational ensemble prediction systems (EPS) and the future of EPS. In: Duan Q et al., eds., Handbook of Hydrometeorological Ensemble Forecasting, Springer: 1–43 .

Chen P Y, Yu H, Xu M, Lei X, Zeng F (2019a). A simplified index to assess the combined impact of tropical cyclone precipitation and wind on China. Front Earth Sci, 13(4): 672–681

Chen L S, Ding Y H (1979). An Introduction to the Western Pacific Typhoon. Beijing: Science Press (in Chinese)

Chen L S, Xu Y L (2017), Review of typhoon very heavy rainfall in China. Meteorol Env S, 40 (1): 3–10 (in Chinese)

Chen L S, Meng Z Y (2001). An overview on tropical cyclone research progress in China during the past ten years. Chin J Atmos Sci, 25(3): 420–432 (in Chinese)

Chen C H, Wang T, Tan Y K, Li C Y, Xu Y C. (2009). Experiments of multi-model short-range ensemble precipitation probability forecasts. J Nanjing Instit Meteor, 32(2): 206–214

Chen G M, Zhang X P, Bai L N, Wan R J. (2019b). Verification on forecasts of tropical cyclones over Western North Pacific and South China Sea in 2017. Meteorol Mon, 45(4): 577–586 (in Chinese)

Craig S S, John S K, Steven J W, Xue M, David R B, Fanyou K, Klein W T, Michael C C, Matthew S W (2010). Toward improved convection-allowing ensembles: model physics sensitivities and optimizing probabilistic guidance with small ensemble membership. Weather Forecast, (25): 263–280

Du J, Mullen S L, Sanders F (1997). Short-range ensemble forecasting (SREF) of quantitative precipitation. Mon Weather Rev, 125(10): 2427–2459

Du J (2002). Present Situation and Prospects of Ensemble Numerical Prediction. J Appl Meteor Sci, 13: 16–28 (in Chinese)

Du J, Zhou B B (2011). A dynamical performance-ranking method for predicting individual ensemble member's performance and its application to ensemble averaging. Mon Weather Rev, 139(10): 3284–3303

Du J, Kang Z M (2014a). A survey on forecasters' view about uncertainty in weather forecasts. Adv Meteorol S, 4(1): 58–67

Du J, Berner J, Buizza R, Charron M, Houtekamer P, Hou D C, Jankov I, Mu M, Wang X G, Wei M Z, Yuan H L (2018). Ensemble methods for meteorological predictions. In: Duan et al., eds. Handbook of Hydrometeorological Ensemble Forecasting, Q. Cham: Springer

Ebert E E (2001a). Ability of a poor man's ensemble to predict the probability and distribution of precipitation. Mon Weather Rev, 129 (10): 2461–2480

Evert E E (2001b). Probability-matched ensemble mean. Available online at CAWCR website

Ebert E E (2008). Fuzzy verification of high resolution gridded forecasts: a review and proposed framework. Meteorol Appl, 15(1): 51–66

Hamill T M, Colucci S J (1997). Verification of Eta–RSM short-range ensemble forecasts. Mon Weather Rev, 125(6): 1312–1327

Hamill T M, Colucci S J (1998). Evaluation of Eta-RSM ensemble probabilistic precipitation forecasts. Mon Wea Rev, 126: 711–724

Hamill T M, Whitaker J S, Fiorino M, Benjamin S G (2010). Global ensemble predictions of 2009's tropical cyclones initialized with an ensemble Kalman Filter. Mon Wea Rev, 139: 668−688

Li J, Du J, Wang M H, Gong Y, Lai A W. (2010). Precipitation verifications to an ensemble prediction system using two initial perturbation schemes based on arem. J Trop Meteorol, 6: 733–742 (in Chinese)

Li J, Du J, Zhang D L, Cui C, Liao Y (2014a). Ensemble-based analysis and sensitivity of mesoscale forecasts of a vortex over southwest China. Q J R Meteorol Soc, 140(680): 766–782

Li J, Du J, Chen C J (2014b). Introduction and analysis to frequency or area matching method applied to precipitation forecast bias correction. Meteorol Mon, 40(5): 580–588 (in Chinese)

Li J, Du J, Chen C J (2015). Applications of 'frequency-matching' method to ensemble precipitation forecasts. Meteorol Mon, 41(6): 674–684 (in Chinese)

Li Z C, Chen D H (2002). The development and application of the operational ensemble prediction system at national meteorological center. J Appl Meteorol Sci, 13(1): 1–15 (in Chinese)

Lorenz E N (1995). The Essence of Chaos. Seatle: University of Washington Press

Lorenz E N (1996). Predictability: a problem partly solved. IN: Proc. Seminar on Predictability, Vol. 1, Reading, United Kingdom, ECMWF, 1–18

Mu M, Zhang Z (2006). Conditional nonlinear optimal perturbations of a two-dimensional quasi-geostrophic model. J Atmos Sci, 63(6): 1587–1604

Murphy A H (1973). A new vector partition of the probability score. J Appl Meteorol, 12(4): 595–600

National Research Council (2006). Completing the Forecast: Characterizing and Communicating Uncertainty for Better Decision Using

Weather and Climate Forecasts. Washington DC: The National Academy Press (USA)

Rosenfeld D, Wolff D B, Atlas D (1993). General probability-matched relations between radar reflectivity and rain rate. J Appl Meteorol, 32 (1): 50–72

Schwartz C S, Kain J S, Weiss S J, Xue M, Bright D R, Kong F, Thomas K W, Levit J J, Coniglio M C, Wandishin M S (2010). Toward improved convection-allowing ensembles: model physics sensitivities and optimizing probabilistic guidance with small ensemble membership. Weather Forecast, 25(1): 263–280

Stensrud D J, Bao J W, Warner T T (2000). Using initial condition and model physics perturbations in short—range ensemble simulations of mesoscale convective systems. Mon Weather Rev, 128(7): 2077–2107

Stefanova L, Krishnamurti T N (2002). Interpretation of seasonal climate forecast using Brier skill score, The Florida State University Superensemble, and the AMIP-I Dataset. J Clim, 15(5): 537–544

Voisin N, Schaake J C, Lettenmaier D P (2010). Calibration and downscaling methods for quantitative ensemble precipitation forecasts. Weather Forecast, 25(6): 1603–1627

Yamaguchi M, Sakai R, Kyoda M, Komori T, Kadowaki T (2009). Typhoon ensemble prediction system developed at the Japan Meteorological Agency. Mon Weather Rev, 137(8): 2592–2604

Yamaguchi M, Nakazawa T, Hoshino S (2012). On the relative benefits of a multi-centre grand ensemble for tropical cyclone track prediction in the western north Pacific. Q J R Meteorol Soc, 138(669): 2019–2029

Yang X S (2001). The new development and the outlook of the operational ensemble prediction system. Meteorol Mon, 27(6): 3–9 (in Chinese)

Yu H, Chen L S (2019). Impact assessment of landfalling tropical cyclones: introduction to the special issue. Front Earth Sci, 13(4): 669–671

Zhi X F, Lyu Y (2019). Calibration of the multimodel precipitation forecasts in China using the frequency matching method. Transac Atmosph Sci, 42(6): 814–823 (in Chinese)

Zhu Y J, Luo Y (2015). Precipitation calibration based on the frequency-matching method. Weather Forecast, 30(5): 1109–1124